

BPAG1e Maintains Keratinocyte Polarity through $\beta 4$ Integrin-mediated Modulation of Rac 1 and Cofilin Activities

Kevin J. Hamill, Susan B. Hopkinson, Philip DeBiase, and Jonathan C.R. Jones

Department of Cell and Molecular Biology, Northwestern University Medical School, Chicago, IL 60611

Submitted January 16, 2009; Revised March 24, 2009; Accepted April 17, 2009
Monitoring Editor: Jean E. Schwarzbauer

$\alpha 6\beta 4$ integrin, a component of hemidesmosomes, also plays a role in keratinocyte migration via signaling through Rac1 to the actin-severing protein cofilin. Here, we tested the hypothesis that the $\beta 4$ integrin-associated plakin protein, bullous pemphigoid antigen 1e (BPAG1e) functions as a scaffold for Rac1/cofilin signal transduction. We generated keratinocyte lines exhibiting a stable knockdown in BPAG1e expression. Knockdown of BPAG1e does not affect expression levels of other hemidesmosomal proteins, nor the amount of $\beta 4$ integrin expressed at the cell surface. However, the amount of Rac1 associating with $\beta 4$ integrin and the activity of both Rac1 and cofilin are significantly lower in BPAG1e-deficient cells compared with wild-type keratinocytes. In addition, keratinocytes deficient in BPAG1e exhibit loss of front-to-rear polarity and display aberrant motility. These defects are rescued by inducing expression of constitutively active Rac1 or active cofilin. These data indicate that the BPAG1e is required for efficient regulation of keratinocyte polarity and migration by determining the activation of Rac1.

INTRODUCTION

$\alpha 6\beta 4$ integrin is a key regulator of epidermal attachment through its function as a surface receptor for laminin-332 (laminin-5) and by nucleating the formation of hemidesmosomes that adhere basal cells in stratified epithelia to the basement membrane (Jones *et al.*, 1991; Dowling *et al.*, 1996; Borradori and Sonnenberg, 1999; Aumailley *et al.*, 2005; Litjens *et al.*, 2006). In addition to its well established role in adhesion, $\alpha 6\beta 4$ integrin has been reported to regulate cell migration and tumor invasion (Rabinovitz and Mercurio, 1996, 1997; Mercurio *et al.*, 2001; Dajee *et al.*, 2003; Nikolopoulos *et al.*, 2004; Nikolopoulos *et al.*, 2005; Sehgal *et al.*, 2006). Moreover, recent data indicate that $\beta 4$ integrin modulates motility via Rac1 signaling to the Slingshot family of phosphatases which dephosphorylate and activate the actin-severing protein cofilin (Sehgal *et al.*, 2006; Kligys *et al.*, 2007).

$\alpha 6\beta 4$ integrin associates with two members of the plakin family of cytoskeletal linker proteins: plectin and bullous pemphigoid antigen 1e (BPAG1e, BP230; Jones *et al.*, 1998; Borradori and Sonnenberg, 1999). This family consists of high-molecular-weight proteins that link cytoskeleton networks and tether cytoskeleton components to the cell surface (Leung *et al.*, 2001). At the site of the hemidesmosome, plectin and BPAG1e proteins anchor the keratin cytoskeleton to the cell surface via $\alpha 6\beta 4$ integrin (Jones *et al.*, 1998;

Borradori and Sonnenberg, 1999). Loss of either BPAG1e or plectin expression in keratinocytes results in the formation of blisters, due to disruption of basal cell/dermal adhesion (Guo *et al.*, 1995; Andra *et al.*, 1997). These data emphasize the importance of plakins in regulating adhesion in the skin. However, BPAG1e-null animals also display impaired wound healing in vivo (Guo *et al.*, 1995). This result indirectly implicates BPAG1e as a potential regulator of keratinocyte migration. This would be consistent with an up-regulation in expression of BPAG1e in invasive squamous cell carcinoma (Herold-Mende *et al.*, 2001). Thus, in our study, we tested the hypothesis that BPAG1e regulates migration by acting as a scaffold for $\beta 4$ integrin-mediated signaling to Rac1.

MATERIALS AND METHODS

Cell Culture, Short Hairpin RNA, Antibodies, and Other Reagents

Human epidermal keratinocytes (HEKs), immortalized with human papilloma virus genes E6 and E7, were described previously (Sehgal *et al.*, 2006). The cells were maintained in defined keratinocyte serum-free medium supplemented with a 1% penicillin/streptomycin mixture (Invitrogen, Carlsbad, CA) and grown at 37°C. Stable short hairpin RNA (shRNA) cell lines were generated using MISSION shRNA lentiviruses (Sigma Aldrich, St. Louis, MO) according to the manufacturer's protocol. Briefly, 5×10^5 HEKs were seeded overnight in six-well dishes and then infected with lentivirus encoding a BPAG1e-specific shRNA (AGTCTTGATTCAAATGAAA) at a multiplicity of infection of 0.5 in culture medium supplemented with Polybrene (8 $\mu\text{g}/\text{ml}$). The following day, the medium of the infected cells was aspirated and replaced with fresh medium containing puromycin (0.5 $\mu\text{g}/\text{ml}$) for selection of stable transfectants. Multiple individual clones were isolated and tested for expression of BPAG1e by SDS-PAGE/immunoblotting and by immunofluorescence.

Mouse monoclonal antibodies against $\beta 4$ integrin (3E1), $\alpha 3$ integrin (P1B5), and Rac1 were purchased from Chemicon International (Temecula, CA). Rabbit monoclonal antibodies against plectin, actin, and paxillin were obtained from Epitomics (Burlingame, CA). Antibodies against tubulin, phospho-cofilin (Ser3), total cofilin, mTor, cytokeratin 5, $\beta 4$ integrin, and the $\beta 3$ laminin subunit were purchased from Novus Biologicals (San Jose, CA), Cell Signaling Technology (Beverly, MA), Abcam (Cambridge, MA), and BD Bio-

This article was published online ahead of print in *MBC in Press* (<http://www.molbiolcell.org/cgi/doi/10.1091/mbc.E09-01-0051>) on April 29, 2009.

Address correspondence to: Jonathan C.R. Jones (j-jones3@northwestern.edu).

Abbreviations used: FRAP, fluorescence recovery after photobleaching; FACS, fluorescent-activated cell sorting; HEK, human epidermal keratinocytes.

sciences (San Jose, CA). 5E, a human mAb against BPAG1e, was a gift from Dr. Takashi Hashimoto (Keio University, Tokyo, Japan; (Hashimoto *et al.*, 1993). The mouse IgM mAb preparation (1804b) against the N-terminal domain of BP180 was described previously, as were antibodies against $\alpha 3$ laminin (RG13) and $\gamma 2$ laminin (3D5; Hopkinson *et al.*, 1992; Goldfinger *et al.*, 1998; Gonzales *et al.*, 1999). Secondary antibodies conjugated with various fluorochromes or horseradish peroxidase were purchased from Jackson ImmunoResearch Laboratories (West Grove, PA).

Adenoviruses expressing constitutively active forms of Rac1, RhoA and Cdc42 and *Xenopus* cofilin were generously provided by Dr. James Bamberg (University of Colorado at Boulder).

Immunoprecipitation and Western Blotting

Cells were extracted in 1% Triton X-100, 25 mM HEPES, pH 7.5, 150 mM NaCl, 5 mM MgCl₂, 2 mM NaF, and 100 μ M Na₃VO₄ supplemented with a protease inhibitor mixture (Sigma-Aldrich). The extract was clarified by centrifugation, and either primary antibody or control IgG was added. After shaking overnight at 4°C, TrueBlot anti-mouse IgG-agarose beads (eBioscience, San Diego, CA) were added to the mix, which was incubated for 90 min at 4°C. The beads were washed, collected by centrifugation, and boiled in SDS-PAGE sample buffer.

Cell extracts and matrix preparations were prepared as described previously (Riddelle *et al.*, 1991; Langhofer *et al.*, 1993). Protein samples were processed for SDS-PAGE and immunoblotting as detailed elsewhere (Harlow and Lane, 1988; Riddelle *et al.*, 1991). Western immunoblots were scanned and quantified using a MetaMorph Imaging System (Universal Imaging, Molecular Devices, Downingtown, PA).

Immunofluorescence Microscopy

Cells on glass coverslips were processed as detailed elsewhere (Sehgal *et al.*, 2006). All preparations were viewed with a confocal laser scanning microscope (UV LSM 510, Zeiss, Thornwood, NY). Images were exported as TIFF files, and figures were prepared using Adobe Photoshop and Illustrator software (Adobe Systems, San Jose, CA).

Observations of Live Cells and Motility Assays

Single-cell motility was measured as detailed by us previously (Sehgal *et al.*, 2006). Briefly, cells were plated onto uncoated 35-mm glass-bottomed culture dishes (MatTek, Ashland, MA) 18–24 h before cell motility assays. Cells were viewed on a Nikon TE2000 inverted microscope (Nikon, Melville, NY). Images were taken at 2 min intervals over 2 h, and cell motility behavior was analyzed by a MetaMorph Imaging System (Universal Imaging, Molecular Devices). Lamellipodia number was quantified by scoring the number of sheet-like extensions in phase-contrast images of live cells. Cell surface area was measured from the same phase-contrast images by tracing the outline of individual cells (including lamellipodia but ignoring filopodia/microspikes and retraction fibers) using MetaMorph Imaging software. Statistical analyses were performed using Microsoft Excel (Redmond, WA), and significance was determined by ANOVA and Student's *t* test as appropriate.

Fluorescent-activated Cell Sorting

For flow cytometry, freshly trypsinized cells were resuspended in phosphate-buffered saline (PBS) containing a 50% dilution of normal goat serum, incubated with monoclonal antibodies against $\alpha 3$ or $\beta 4$ integrin for 45 min at room temperature, washed with PBS, incubated with FITC-conjugated goat anti-mouse IgG for 45 min, washed, resuspended in PBS, and analyzed using a Beckman Coulter Elite PCS sorter (Beckman Coulter, Fullerton, CA). For negative controls, primary antibody was omitted from the above procedure.

Rac GLISA

Quantitative analysis of Rac activation was performed using a GLISA Rac activation assay (Cytoskeleton, Denver, CO). Briefly, cell lysates were prepared from HEKs or HEK293s at 50% confluence, and their protein concentration was normalized. Samples at a protein concentration of 2 mg/ml in 96-well plate format were used for determination of Rac activity according to the manufacturer's instructions using an ELx808 ultramicroplate spectrophotometer (Bio-Tek Instruments, Winooski, VT). Data analyses were performed using Microsoft Excel.

Fluorescence Recovery after Photobleaching

Fluorescence recovery after photobleaching (FRAP) studies were performed as described elsewhere (Tsuruta *et al.*, 2002, 2003). Briefly, HEKs or HEK293s were infected with retrovirus encoding green fluorescent protein (GFP)-tagged, full-length $\beta 4$ integrin (Sehgal *et al.*, 2006). Time-lapse observations were made using a UV LSM 510 confocal microscope (Zeiss) under the following conditions: 100 \times , 1.4 NA oil immersion objective, maximum power 25 mW, tube current 5.1 A (31% laser power), and pinhole 1.33 airy units (optical slice, 1.0 μ m). GFP images were acquired by excitation at 488 nm and emission at 515–545 nm. Cell regions were bleached at the plane of the membrane at 488 nm, 100% laser power using the minimum number of iterations to cause complete bleaching ($n = 20$ –40). Recovery was monitored at 31% laser power at 1-min intervals. For quantitative analyses, the fluorescence intensity of 1) the photobleached region, 2) the extracellular background intensity, and 3) intracellular brightest intensity were determined using MetaMorph 4.0 software (Universal Imaging). All data were analyzed using Microsoft Excel. Data were adjusted for sample fading as detailed elsewhere (Tsuruta *et al.*, 2002, 2003).

RESULTS

BPAG1e Colocalizes with $\beta 4$ Integrin at the Leading Edge of Migrating Keratinocytes

There is accumulating evidence that $\beta 4$ integrin is involved in keratinocyte migration (Rabinovitz and Mercurio, 1997; Mercurio *et al.*, 2001; Nikolopoulos *et al.*, 2004, 2005; Pullar *et al.*, 2006; Sehgal *et al.*, 2006). To test for an association between $\beta 4$ integrin and BPAG1e in actively migrating cells, we created a scratch wound in a confluent monolayer of HEKs. The cells surrounding the scratch were allowed to

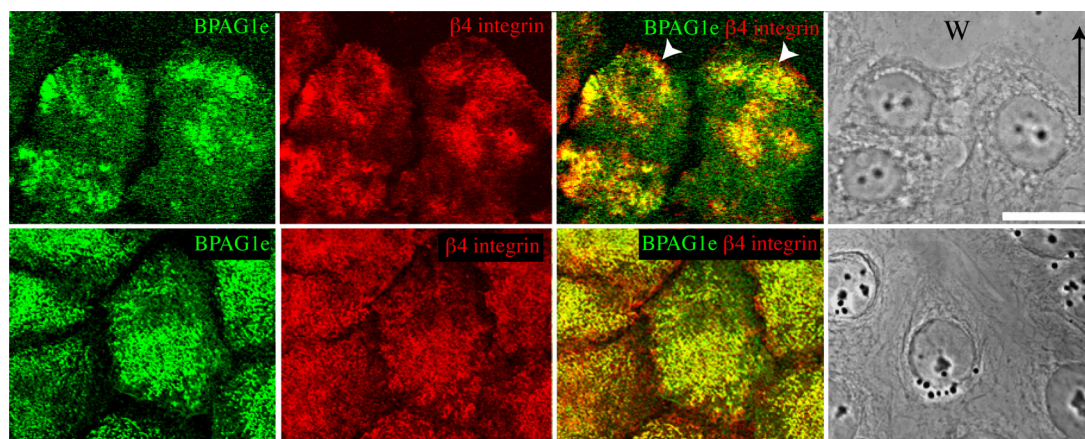


Figure 1. BPAG1e and $\beta 4$ integrin colocalize at the leading edge of migrating epithelial sheets. A scratch wound was introduced into a confluent monolayer of HEKs. The monolayer was allowed to reclose for 6 h and then was fixed and prepared for indirect immunofluorescence microscopy with antibodies against BPAG1e and $\beta 4$ integrin as indicated. Top panels, cells migrating into the scratched area; bottom panels, cells distant from the wound site. W and arrow in the phase image in the top panel mark the wound site and direction of migration, respectively. Bar, 20 μ m.

migrate into the wounded region for 6 h and subsequently were prepared for immunofluorescence microscopy using BPAG1e and $\beta 4$ integrin probes. There is extensive colocalization of BPAG1e and $\beta 4$ integrin not only along the basal aspect of the essentially stationary cells distant from the wound margin, but also toward the leading front of the cells

migrating into the scratch site (Figure 1). These results suggest that BPAG1e may function in concert with $\beta 4$ integrin to regulate keratinocyte motility.

Lentiviral-mediated shRNA Knockdown of BPAG1e in Epidermal Keratinocytes

To evaluate the effect of BPAG1e on keratinocyte migration, BPAG1e expression was reduced in HEKs using lentiviral mediated delivery of shRNA targeting the BPAG1e message. Protein extracts, generated from the multiple clones, were then processed for immunoblotting using BPAG1e antibody. The expression levels of BPAG1e in the selected clones range from 26 to 76% relative to HEKs (Figure 2A). In subsequent experiments we used clone 2 cells (HEKCn2s) and clone 12 cells (HEKCn12s) whose expression of BPAG1e is 26 and 48%, respectively, of the level in HEKs.

To determine if BPAG1e knockdown affects the expression levels of other hemidesmosomal components, extracts of HEKCn2s were prepared for immunoblotting using BP180 (bullous pemphigoid antigen 2 [BPAG2]), plectin, and $\beta 4$ integrin antibodies (Figure 2B). Extracellular matrix protein extracts of the cells were probed likewise for the subunits of laminin-332 ($\alpha 3$, $\beta 3$, and $\gamma 2$; Figure 2C). No change in protein levels is observed in any instance. Furthermore, cell surface proteins were biotin labeled, pulled down with

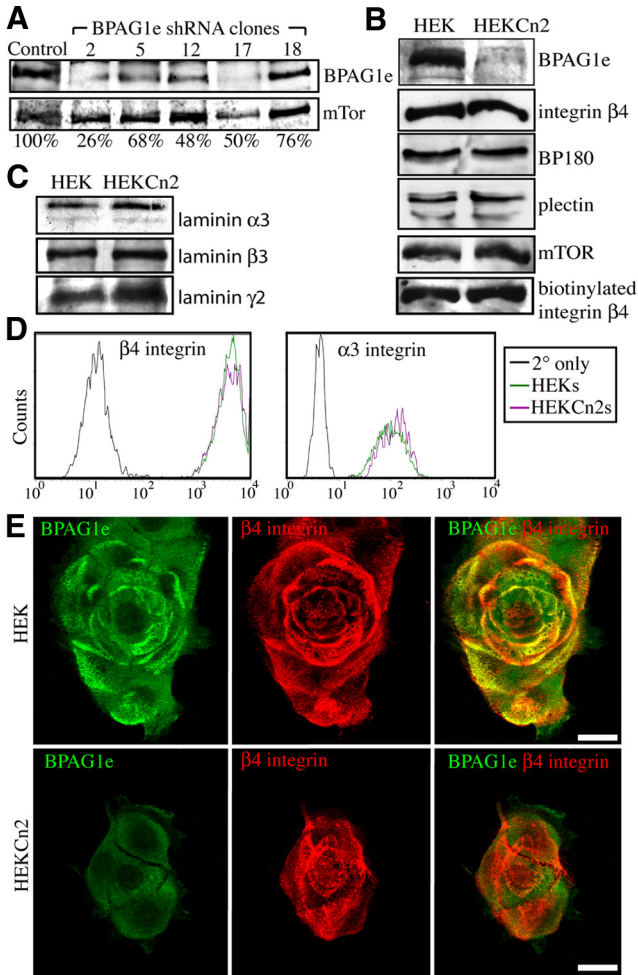


Figure 2. Generation of keratinocytes deficient in BPAG1e expression. (A) HEKs were infected with a lentivirus encoding shRNA targeting BPAG1e. Total cell lysates from a number of different stable clones were prepared for SDS-PAGE/immunoblotting and then probed with BPAG1e and mTOR antibodies as shown. The percentage expression of BPAG1e in clones 2, 5, 12, 17, and 18 relative to HEKs (Control) was calculated after densitometric scanning of the blots and is indicated underneath each lane. (B) Cell lysates from HEKs and HEK clone 2 cells (HEKCn2s) were probed in immunoblots with antibodies against BPAG1e, BP180, plectin, and $\beta 4$ integrin as marked. In the bottom immunoblot in B, cell surface proteins that had been biotinylated and subsequently immunoprecipitated by streptavidin-coated beads were probed with antibodies against $\beta 4$ integrin. (C) Extracellular matrix preparations of the HEKs and HEKCn2s were probed in immunoblots with antibodies specific for the $\alpha 3$, $\beta 3$, and $\gamma 2$ laminin subunits. (D) Cell-surface expression of $\beta 4$ integrin and $\alpha 3$ integrin was compared in HEKs and HEKCn2s by FACS as indicated (black tracing; secondary antibody alone). (E) HEKs and HEKCn2s were plated onto glass coverslips. Forty-eight hours later the cells were fixed and prepared for double-label immunofluorescence microscopy with a mix of antibodies against BPAG1e and $\beta 4$ integrin, as indicated. In the right-hand column, the separate green and red fluorescence images are overlaid. Bars, 20 μm .

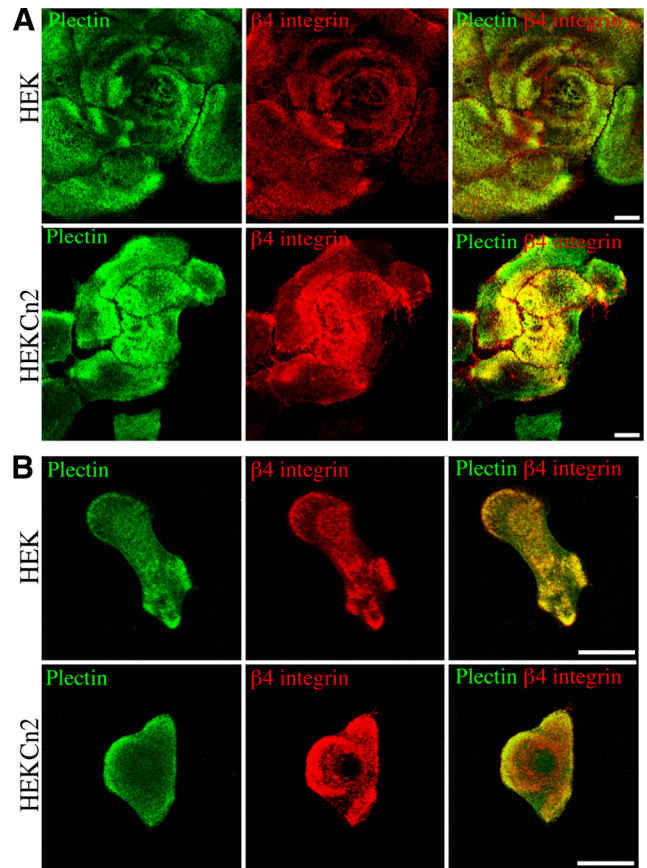


Figure 3. Plectin and $\beta 4$ integrin colocalization in keratinocytes is not dependent on BPAG1e. HEKs and HEKCn2s were plated onto glass coverslips and 48 (A) or 24 h (B) later were fixed and then imaged by confocal immunofluorescence microscopy after staining with antibodies against plectin and $\beta 4$ integrin, as indicated. Red and green images are shown overlaid in the right-hand column. Bars, 20 μm .

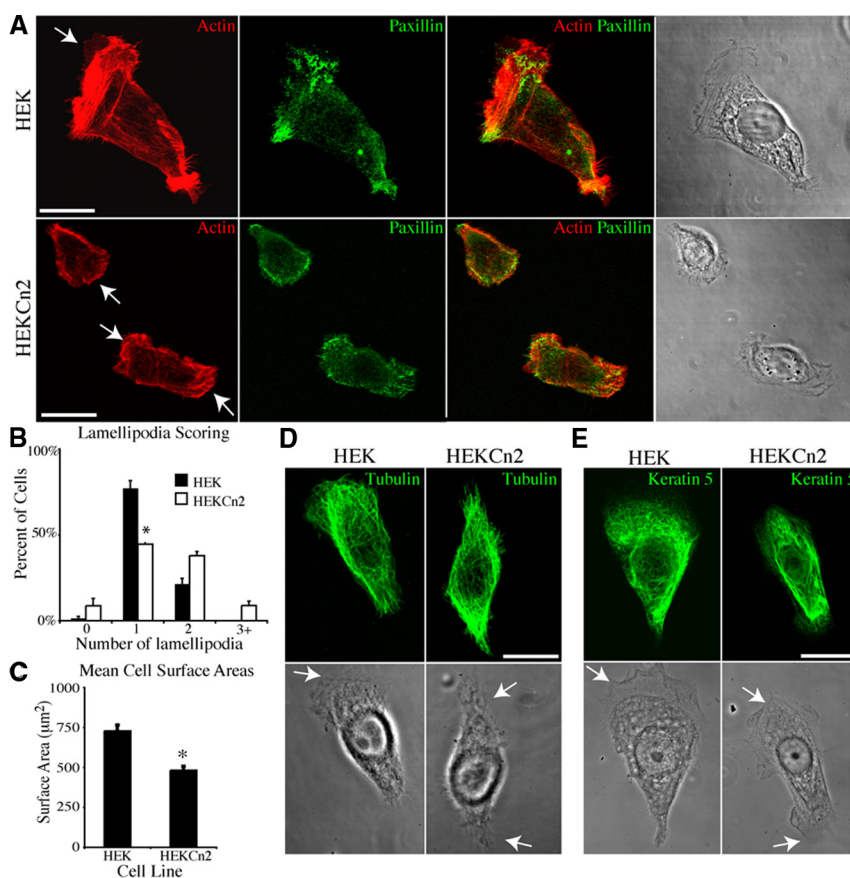


Figure 4. Cell surface area and cytoskeleton localization are perturbed in keratinocytes deficient in BPAG1e. (A) HEKs and HEKcN2s were plated onto glass coverslips and 24 h later were fixed and stained with for double-labeling with rhodamine-conjugated phalloidin and antibodies against paxillin. Arrows in A, D, and E indicate lamellipodia. More than 50 live cells in each of three trials were scored for the number of lamellipodia that each displays. Lamellipodia scores are graphed in B (graph represents mean \pm SEM). The percentage of HEKs exhibiting a single lamellipodium is higher than in HEKcN2s (* $p < 0.019$). (C) HEKs and HEKcN2s were plated onto uncoated glass coverslips, and 24 h later cell surface area was measured using Metamorph software. More than 50 cells were evaluated per trial in three trials. HEKcN2s are slightly smaller than HEKs (* $p < 0.01$). (D and E) HEKs and HEKcN2s were plated onto glass coverslips and 24 h later were fixed and stained with antibodies against γ -tubulin (D) or cytokeratin 5 (E). The cells were then imaged by confocal microscopy. Bars, 20 μ m.

streptavidin-conjugated beads, and probed for $\beta 4$ integrin. HEKcN2s exhibit no reduction in cell surface levels of $\beta 4$ integrin (Figure 2B, bottom panel). This result was confirmed by FACS analysis, which also demonstrates that $\alpha 3$ integrin cell surface expression is similar in HEKs and HEKcN2s (Figure 2D).

Subconfluent (60–80%) HEKs and HEKcN2s were analyzed by immunofluorescence microscopy for BPAG1e expression. Whereas control cells exhibit BPAG1e staining in arcs and rosette-like patterns that colocalize with $\beta 4$ integrin along their substratum-attached surface, there is barely detectable BPAG1e antibody staining in HEKcN2s (Figure 2E). In HEKcN2s $\beta 4$ integrin staining is observed in the same overall patterns seen in HEKs (Figure 2E).

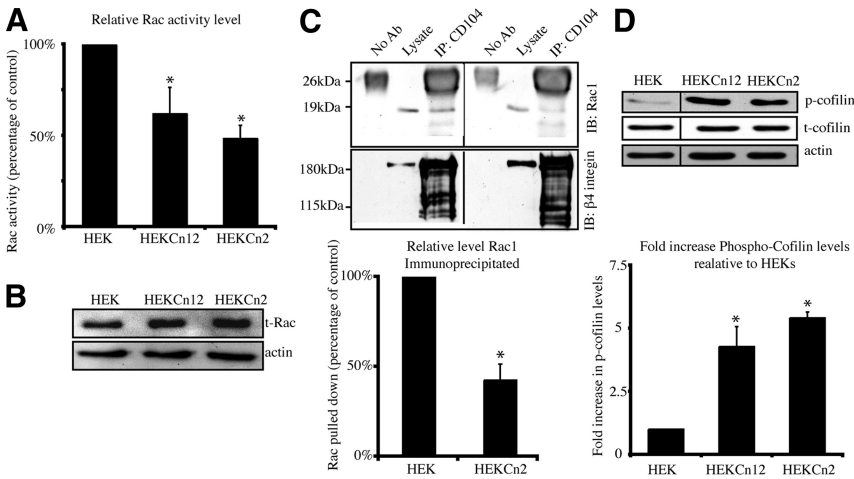
$\beta 4$ integrin interacts with two plakin family members, namely BPAG1e and plectin (Hopkinson and Jones, 2000). Thus, we evaluated whether a loss in expression of BPAG1e impacts $\beta 4$ integrin association with plectin. Comparison of staining patterns for plectin in HEKcN2s versus HEKs reveals that plectin localization is not perturbed in near confluent cells as a result of BPAG1e knockdown and is colocalized with $\beta 4$ integrin (Figure 3A). We also compared staining for plectin and $\beta 4$ integrin in single, motile HEKs and HEKcN2s. In both, plectin and $\beta 4$ integrin colocalize, particularly at the edges of cells (Figure 3B).

BPAG1e Knockdown Leads to Rearrangement of the Actin Cytoskeleton, Changes in Focal Contact Protein Distribution, Reduced Cell Surface Area, and Loss of Front/Rear Polarity

The immunofluorescence images in Figures 2 and 3 indicate that HEKcN2s are smaller and exhibit a loss in front/rear

polarity, suggesting that BPAG1e deficiency impacts cytoskeletal organization. HEKs and HEKcN2s were therefore prepared for immunofluorescence to assess their cytoskeletal organization. In the majority of HEKs, F-actin is organized in a tight bundle just distal to a fan-like, polarized lamellipodium (Figure 4A, top panels). Retraction fiber-like structures are present on the opposing side of such HEKs (Figure 4A, top panels). In contrast, HEKcN2s prepared for F-actin staining exhibit multiple phenotypes, with a far greater proportion of cells displaying two or more lamellipodia (Figure 4A, bottom panels). Focal contact organization is also perturbed in HEKcN2s when compared with HEKs, as evidenced by immunofluorescence localization of paxillin. Paxillin is organized into distinct puncta, primarily decorating the leading edge of HEKs (Figure 4A). In contrast, in the majority of HEKcN2s, paxillin is found around the edges of their multiple lamellipodia, and frequently fails to resolve into discrete puncta (Figure 4A).

To quantify these observed differences in front/rear polarity and cell surface area, phase-contrast images were taken of live cells, and the number of sheet-like extensions (lamellipodia) was scored. This reveals that significantly fewer HEKcN2s display a single lamellipodia compared with HEKs (graphed in Figure 4B, see also Supplemental Figure S1 for examples of scoring). In addition, the surface area of HEKcN2s is slightly, but significantly, less than HEKs (Figure 4C). This difference in cell spreading may reflect changes in cytoskeletal/focal adhesion organization in the knockdown cells (Figure 4A). There is no obvious difference in the microtubule or keratin networks of HEKcN2s when compared with HEKs (Figure 4, D and E).



HEKcN12s were prepared for immunoblotting using antibodies specific for Ser-3-phosphorylated cofilin or F-actin. Blots were densitometrically scanned, the levels were normalized to actin, and the fold increase of phosphorylated cofilin, relative to the level in HEKs, was quantified. The graph beneath the blot displays the mean \pm SEM in three independent trials (significance relative to HEKs; * $p < 0.05$).

Rac1 and Cofilin Activity Levels Are Reduced in BPAG1e Knockdown Cells

The above data indicate that loss of BPAG1e in keratinocytes impacts lamellipodia formation, polarity, and actin cytoskeleton organization. The small Rho GTPase Rac is known to be involved in each of these events. Because $\beta 4$ integrin regulates Rac activity, we next assayed the levels of active Rac1 in HEKs, HEKcN2s, and HEKcN12s using a Rac G-LISA (Russell *et al.*, 2003; Zahir *et al.*, 2003; Sehgal *et al.*, 2006; Figure 5A). Rac 1 activity is significantly lower in both knockdown clones than in HEKs (Figure 5A). Specifically, Rac1 activity is decreased by 51% in HEKcN2s and by 38% in HEKcN12s. Blotting for total Rac1 in lysates from HEK, HEKcN2s, and HEKcN12s revealed that the observed change in activity levels is not due to a change in Rac1 expression levels but rather is a change in Rac1 activity (Figure 5B).

Previously, we demonstrated that Rac1 coprecipitates with $\alpha 6\beta 4$ integrin in HEKs (Sehgal *et al.*, 2006). Thus, we investigated if this interaction is perturbed in HEKcN2s. There is a significant decrease in the levels of Rac1 that coimmunoprecipitates with $\beta 4$ from extracts of HEKcN2s compared with that coprecipitated with $\beta 4$ integrin from HEKs (Figure 5C). Together with the Rac activation assay detailed above, our data implicate BPAG1e as being necessary for the activation of Rac1 by $\alpha 6\beta 4$ integrin.

In HEKs, Rac activation leads to dephosphorylation of the actin-severing protein cofilin (Sehgal *et al.*, 2006; Kligys *et al.*, 2007). Thus, we analyzed extracts of HEKs, HEKcN2s, and HEKcN12s for the presence of inactivated (serine-3 phosphorylated) cofilin (Soosairajah *et al.*, 2005). Our data indicate that there are significantly higher levels of inactive, phosphorylated cofilin in HEKcN2s and HEKcN12s compared with that of HEKs (Figure 5D).

BPAG1e Knockdown Cells Show Aberrant Motility Patterns Relative to Controls

On the basis of the changes that we have observed in the front/rear polarity of HEKcN2, we hypothesized that this would likely result in a motility defect. To address this possibility, we evaluated the motile behavior of HEKs and HEKcN2s in single-cell assays (Sehgal *et al.*, 2006; Kligys

et al., 2007). HEKs generally migrate either back and forth over linear trails or in a persistent manner, whereas HEKcN2s display frequent turning in their migration patterns, often exhibiting circular migration behavior (Figure 6, A and B; Supplemental Videos 1 and 2). The motility defect of HEKcN12s is less severe than HEKcN2s consistent with the less efficient knock down in BPAG1e expression detected in HEKcN12s (Figure 6C).

Expression of Constitutively Active Rac1 or Cofilin Rescues the Motility of HEKs Exhibiting BPAG1e Knockdown

If the motility behavior of HEKcN2s is dependent on Rac1 and cofilin activity, expression of constitutively active Rac1 or cofilin would be predicted to restore normal migration of HEKcN2s. To test this hypothesis, HEKcN2s were infected with adenoviruses engineered to express constitutively active Rac1, RhoA, or Cdc42 along with a GFP moiety. The migration patterns of labeled cells were then quantified. HEKcN2s expressing constitutively active Rac1 move back and forth in patterns comparable to HEKs, whereas there is no "rescue" of the motility defect of HEKcN2s expressing constitutively active RhoA or Cdc42 (Figure 6, D–F, graphed in H). The motility defect of HEKcN2s is also rescued by inducing the expression of active cofilin (Figure 6, G and H). Notably, differences in migration rates between all cell lines/treatments were below significance, suggesting that the motility defect of BPAG1e-deficient cells is likely in establishment or maintenance of front/rear polarity as opposed to a defect in motility per se (Figure 6I).

$\beta 4$ Integrin Dynamics Are Reduced in Migratory HEKs Exhibiting BPAG1e Knockdown

Previously, we demonstrated that $\beta 4$ integrin dynamics are enhanced upon actin depolymerization, suggesting that actin acts as a brake on the movement of $\alpha 6\beta 4$ integrin complexes in the plane of the membrane (Tsuruta *et al.*, 2003). We also have suggested that cofilin activity is involved in this phenomenon (Sehgal *et al.*, 2006). Thus, we reasoned that a decrease in cofilin activity might change $\beta 4$ integrin dynamics in keratinocytes. Therefore, we retrovirally infected HEKs and HEKcN2s with GFP-tagged $\beta 4$ integrin

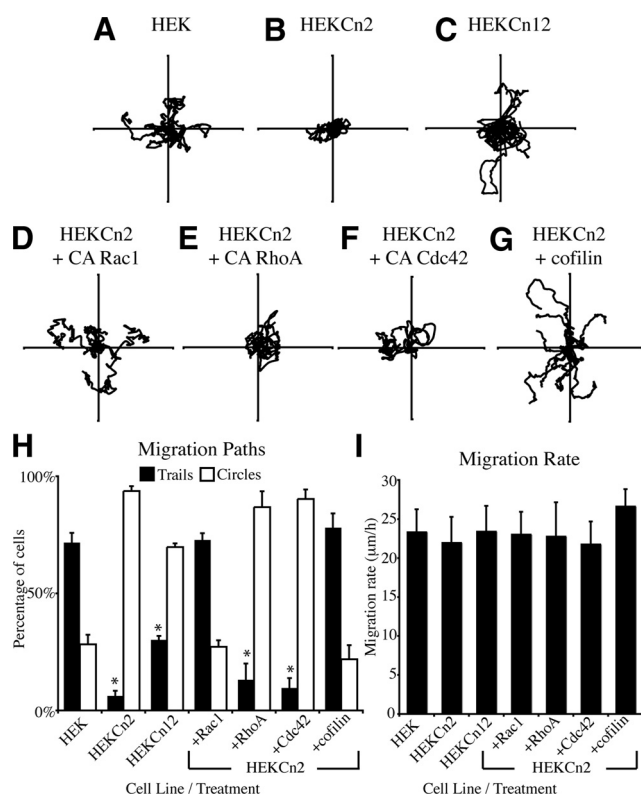


Figure 6. Constitutively active Rac1 and cofilin rescue motility defects of keratinocytes deficient in BPAG1e. HEKs (A, Supplemental Video 1) HEKCn2s (B, Supplemental Video 2), HEKCn12s (C), and HEKCn2s infected with adenovirus encoding constitutively active forms of Rac1 (D), RhoA (E), Cdc42 (F), or cofilin (G) were plated onto uncoated glass-bottomed dishes, and 16 h later motility patterns of individual cells were tracked over a 2 h period. Virally infected cells were identified by visualizing GFP. Vector diagrams show the migration pattern of 10 cells, with each line representing the migration of a single cell. (H) Cells from a minimum of four trials per treatment, with a minimum of 10 cells tracked per trial, were scored as trails (■) if they migrated in a predominantly linear and/or backtracking manner or circles (□) if they moved over an approximately circular track and were plotted as percentage of total. The percentage of HEKCn2s moving in a trail under each condition was compared with the percentage of HEKs moving in a similar manner (* $p < 0.01$). (I) Migration rates for cells visualized in A–G were calculated by summing the displacement of cell bodies between each time point in order to calculate total displacement over time. Differences between cell lines/infections were below significance.

and assayed $\beta 4$ dynamics by FRAP at both the leading edge of cells moving into scratch wounds and in stationary cells (representative images Figure 7, A and B). Consistent with reduced cofilin activity and a consequent reduced actin remodeling, $\beta 4$ dynamics at the leading edge of migrating HEKCn2s is reduced compared with that observed in HEKs (Figure 7, A and B, graphed in C). In contrast, there is no significant difference in $\beta 4$ integrin dynamics in confluent, nonmigratory HEKs and HEKCn2s, as determined by FRAP (Figure 7, A and B, graphed in C).

DISCUSSION

The importance of $\alpha 6\beta 4$ integrin in keratinocyte adhesion is well established and has been extensively studied (Jones *et al.*, 1994, 1998; Borradori and Sonnenberg, 1996; Nievers

et al., 1999). Indeed, the skin fragility disorders of the epidermolysis bullosa family exemplify the importance of the linkage from extracellular laminin 332 to intracellular keratin 5/14 provided by $\alpha 6\beta 4$ integrin and its plakin-binding partners BPAG1e and plectin (Christiano and Uitto, 1996; Pulkkinen and Uitto, 1999). In contrast, the role of integrins in regulating keratinocyte motility on laminin matrices is controversial. A number of workers have proposed that $\alpha 3\beta 1$ integrin mediates migration on laminin 332, whereas recent data indicate that $\alpha 3\beta 1$ may actually act to retard keratinocyte motility (Hodivala-Dilke *et al.*, 1998; Hintermann *et al.*, 2001; Margadant *et al.*, 2009). Moreover, although it has been reported that $\alpha 6\beta 4$ integrin negatively regulates migration there is accumulating evidence that, under certain circumstances, $\alpha 6\beta 4$ integrin activates migration promoting signaling pathways (Mercurio *et al.*, 2001; deHart *et al.*, 2003; Raymond *et al.*, 2005; Sehgal *et al.*, 2006). In addition, although keratinocytes genetically null for $\beta 4$ integrin close epithelial wounds more slowly than their wild-type counterparts, $\alpha 3$ integrin-null epidermal cells display enhanced wound closure rates (deHart *et al.*, 2003; Russell *et al.*, 2003; Sehgal *et al.*, 2006; Reynolds *et al.*, 2008; Margadant *et al.*, 2009). Furthermore, previous studies have demonstrated that keratinocytes deficient in $\beta 4$ integrin exhibit reduced Rac activity, which leads to their aberrant motility (Russell *et al.*, 2003; Pullar *et al.*, 2006; Sehgal *et al.*, 2006). However, the precise mechanics of the link from $\beta 4$ integrin to Rac activity have yet to be fully elucidated.

Here, we provide evidence that the plakin molecule BPAG1e mediates $\beta 4$ integrin regulation of Rac1 activity and is an essential component of the signaling pathway via which $\beta 4$ integrin determines both cell front/rear polarity and processivity of cell migration. That BPAG1e does so is an unanticipated function for this plakin protein family member that has been thought to be purely a structural linker protein. Indeed, our data now imply that BPAG1e is also a signal scaffold protein, in addition to its ability to interact with and organize the keratin cytoskeleton. In this regard, we do not yet know whether BPAG1e binds Rac1 directly or whether it somehow modulates the association of Rac1 with $\alpha 6\beta 4$ integrin complexes at the cell surface. This will be an interesting avenue of investigation for the future.

Another plakin molecule, namely plectin, also binds $\beta 4$ integrin and is already known to interact with a number of signaling molecules/complexes (Andra *et al.*, 1998; Osmanagic-Myers and Wiche, 2004; Osmanagic-Myers *et al.*, 2006). However, our results clearly indicate that plectin cannot compensate for the loss of BPAG1e in keratinocytes, at least with regard to Rac1 and cofilin activation, processivity of migration, or the determination of front/rear polarity.

The dynamics of integrin clusters in the plane of the substrate-attached cell membrane are known to play an important role in regulating cellular adhesion and migration (Palecek *et al.*, 1996; Smilenov *et al.*, 1999; Geuijen and Sonnenberg, 2002; Wiseman *et al.*, 2004). In the studies described here we report that in stationary cells $\beta 4$ integrin is significantly less dynamic than in migrating cells. This is not surprising because, in nonmotile cells, $\alpha 6\beta 4$ integrin is likely incorporated into hemidesmosome-like stable anchoring contacts, which interact with the keratin cytoskeleton (Jones *et al.*, 1991, 1998). The finding that $\beta 4$ integrin dynamics in stationary cells is unaffected by BPAG1e expression levels is somewhat more surprising because one might assume that the loss of this keratin-binding protein might result in an increase in integrin dynamics in the plane of the membrane. However, we also present evidence that plectin association with $\alpha 6\beta 4$ is retained in confluent, nonmigratory BPAG1e-

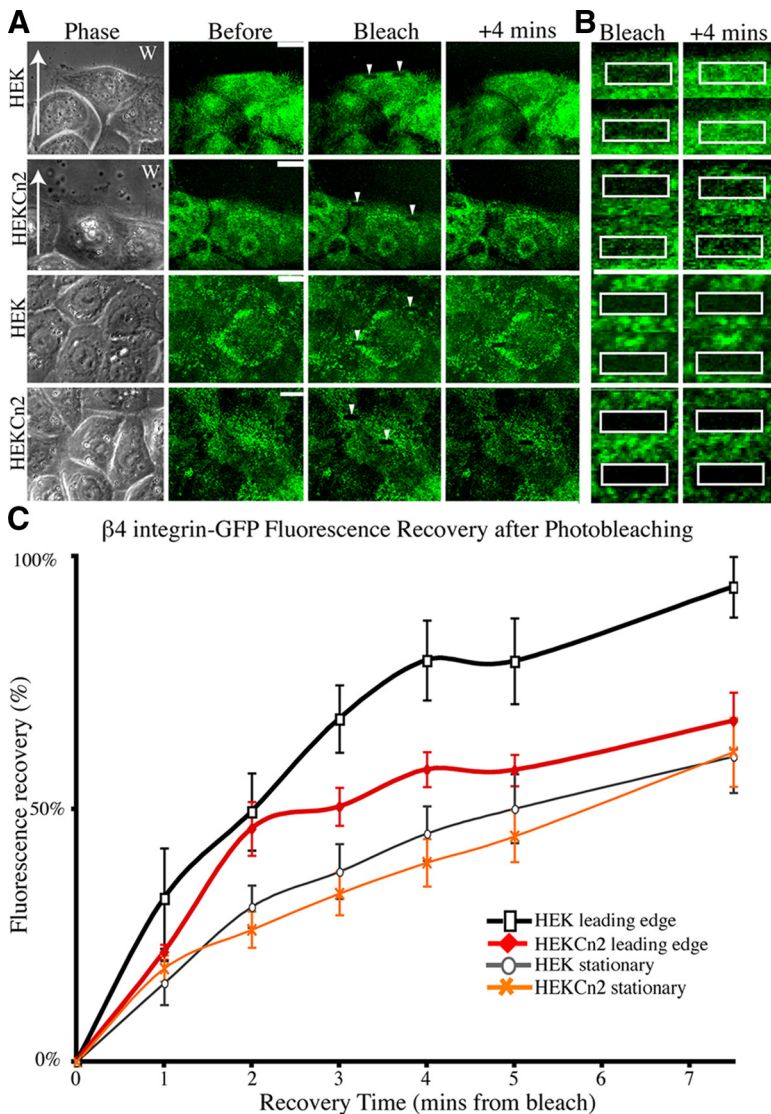


Figure 7. Dynamics of $\beta 4$ integrin in keratinocytes deficient in BPAG1e. HEKs or HEKcN2s were infected with retrovirus encoding GFP-tagged $\beta 4$ integrin. FRAP of the arrowed boxes (images of these bleached areas are shown at higher magnification in B) was measured either at the leading edge of cells migrating into a scratch wound (A and B, two top panels; C, black/red lines; arrows indicate direction of migration) or in stationary cells close to or at confluence (A and B, two bottom panels; C, gray/orange lines). Fluorescence recovery is plotted as a percentage of the prebleach levels, allowing for background fading. The graph in C represents mean \pm SEM; $n = 8$.

deficient cells. Thus, plectin likely stabilizes $\alpha 6\beta 4$ integrin dynamics in such cells by providing a link from $\beta 4$ to the keratin cytoskeleton. Consistent with this, immunofluorescence staining for keratin 5 in BPAG1e-deficient cells reveals very little difference in keratin intermediate filament organization.

We observe a significant increase in $\beta 4$ integrin dynamics at the leading edge of migrating keratinocytes. We speculate that $\beta 4$ dynamics are likely to be dependent on localized actin remodeling, leading to a locally permissive environment for $\beta 4$ integrin movement in the plane of the membrane. Consistent with this premise, we have previously reported that depolymerization of actin, through treatment with cytochalasin D, actually enhances $\beta 4$ integrin dynamics (Tsuruta *et al.*, 2003). Moreover, we report here that there is a significant reduction in $\beta 4$ integrin dynamics at the leading edge of BPAG1e-deficient keratinocytes. These data suggest that at the leading edge of migrating cells the recruitment by BPAG1e of Rac1 and cofilin to the cell surface, and their consequent activation leads to localized remodeling of the actin cytoskeleton that releases a brake on the movement of $\alpha 6\beta 4$ integrin complexes in the plane of the membrane.

The reduction in $\beta 4$ dynamics in BPAG1e-deficient cells may, in part, explain the loss of their processivity of migration. We speculate that there is a feedback loop in which a complex of $\beta 4$ integrin/BPAG1e activates Rac1 and cofilin, whose activity then drives lamellipodia formation through actin remodeling. The latter, in turn, releases the cytoskeleton brake on $\alpha 6\beta 4$ dynamics, inducing integrin clustering and stabilization of the newly formed lamellipodia (Santoro *et al.*, 2003). Consistent with this model, expression of active Rac1 or cofilin can bypass the requirement for BPAG1e in the presence but not absence of $\beta 4$ integrin (Pullar *et al.*, 2006; Sehgal *et al.*, 2006).

In summary, our data provide new mechanistic insight into the wound-healing defect observed in BPAG1e-null mouse skin *in vivo* (Guo *et al.*, 1995). BPAG1e is clearly multifunctional in keratinocytes. In the cells in the basal layer of an intact epidermis, BPAG1e is part of a complex mediating stable adhesion of cells to the extracellular matrix. However, BPAG1e also has an important function during wound healing and possibly tumorigenesis as a regulator of cell polarity and migration.

ACKNOWLEDGMENTS

We thank Dr. James Bamburg for generously donating reagents. This work was supported by National Institutes of Health Grant RO1 AR054184 (J.C.R.J.).

REFERENCES

- Andra, K., Lassmann, H., Bittner, R., Shorny, S., Fassler, R., Propst, F., and Wiche, G. (1997). Targeted inactivation of plectin reveals essential function in maintaining the integrity of skin, muscle, and heart cytoarchitecture. *Genes Dev.* *11*, 3143–3156.
- Andra, K., Nikolic, B., Stocher, M., Drenckhahn, D., and Wiche, G. (1998). Not just scaffolding: plectin regulates actin dynamics in cultured cells. *Genes Dev.* *12*, 3442–3451.
- Aumailley, M., et al. (2005). A simplified laminin nomenclature. *Matrix Biol.* *24*, 326–332.
- Borradori, L., and Sonnenberg, A. (1996). Hemidesmosomes: roles in adhesion, signaling and human diseases. *Curr. Opin. Cell Biol.* *8*, 647–656.
- Borradori, L., and Sonnenberg, A. (1999). Structure and function of hemidesmosomes: more than simple adhesion complexes. *J. Invest. Dermatol.* *112*, 411–418.
- Christiano, A. M., and Uitto, J. (1996). Molecular complexity of the cutaneous basement membrane zone. Revelations from the paradigms of epidermolysis bullosa. *Exp. Dermatol.* *5*, 1–11.
- Dajee, M., et al. (2003). NF-kappaB blockade and oncogenic Ras trigger invasive human epidermal neoplasia. *Nature* *421*, 639–643.
- deHart, G. W., Healy, K. E., and Jones, J. C. (2003). The role of alpha3beta1 integrin in determining the supramolecular organization of laminin-5 in the extracellular matrix of keratinocytes. *Exp. Cell Res.* *283*, 67–79.
- Dowling, J., Yu, Q. C., and Fuchs, E. (1996). Beta4 integrin is required for hemidesmosome formation, cell adhesion and cell survival. *J. Cell Biol.* *134*, 559–572.
- Geuijen, C. A., and Sonnenberg, A. (2002). Dynamics of the alpha6beta4 integrin in keratinocytes. *Mol. Biol. Cell* *13*, 3845–3858.
- Goldfinger, L. E., Stack, M. S., and Jones, J. C. (1998). Processing of laminin-5 and its functional consequences: role of plasmin and tissue-type plasminogen activator. *J. Cell Biol.* *141*, 255–265.
- Gonzales, M., Haan, K., Baker, S. E., Fitchmun, M., Todorov, I., Weitzman, S., and Jones, J. C. (1999). A cell signal pathway involving laminin-5, alpha3beta1 integrin, and mitogen-activated protein kinase can regulate epithelial cell proliferation. *Mol. Biol. Cell* *10*, 259–270.
- Guo, L., Degenstein, L., Dowling, J., Yu, Q. C., Wollmann, R., Perman, B., and Fuchs, E. (1995). Gene targeting of BPAG 1, abnormalities in mechanical strength and cell migration in stratified epithelia and neurologic degeneration. *Cell* *81*, 233–243.
- Harlow, E., and Lane, D. (1988). *Antibodies: A Laboratory Manual*, Cold Spring Harbor, NY: Cold Spring Harbor Laboratory Press.
- Hashimoto, T., Amagai, M., Ebihara, T., Gamou, S., Shimizu, N., Tsubata, T., Hasegawa, A., Miki, K., and Nishikawa, T. (1993). Further analyses of epitopes for human monoclonal anti-basement membrane zone antibodies produced by stable human hybridoma cell lines constructed with Epstein-Barr virus transformants. *J. Invest. Dermatol.* *100*, 310–315.
- Herold-Mende, C., Kartenbeck, J., Tomakidi, P., and Bosch, F. X. (2001). Metastatic growth of squamous cell carcinomas is correlated with upregulation and redistribution of hemidesmosomal components. *Cell Tissue Res.* *306*, 399–408.
- Hintermann, E., Bilban, M., Sharabi, A., and Quaranta, V. (2001). Inhibitory role of alpha 6 beta 4-associated erbB-2 and phosphoinositide 3-kinase in keratinocyte haptotactic migration dependent on alpha 3 beta 1 integrin. *J. Cell Biol.* *153*, 465–478.
- Hodivala-Dilke, K. M., DiPersio, C. M., Kreidberg, J. A., and Hynes, R. O. (1998). Novel roles for alpha3beta1 integrin as a regulator of cytoskeletal assembly and as a trans-dominant inhibitor of integrin receptor function in mouse keratinocytes. *J. Cell Biol.* *142*, 1357–1369.
- Hopkinson, S. B., and Jones, J. C. (2000). The N terminus of the transmembrane protein BP180 interacts with the N-terminal domain of BP230, thereby mediating keratin cytoskeleton anchorage to the cell surface at the site of the hemidesmosome. *Mol. Biol. Cell* *11*, 277–286.
- Hopkinson, S. B., Riddelle, K. S., and Jones, J. C. (1992). Cytoplasmic domain of the 180-kD bullous pemphigoid antigen, a hemidesmosomal component: molecular and cell biologic characterization. *J. Invest. Dermatol.* *99*, 264–270.
- Jones, J. C., Asmuth, J., Baker, S. E., Langhofer, M., Roth, S. I., and Hopkinson, S. B. (1994). Hemidesmosomes: extracellular matrix/intermediate filament connectors. *Exp. Cell Res.* *213*, 1–11.
- Jones, J. C., Hopkinson, S. B., and Goldfinger, L. E. (1998). Structure and assembly of hemidesmosomes. *Bioessays* *20*, 488–494.
- Jones, J. C., Kurpakus, M. A., Cooper, H. M., and Quaranta, V. (1991). A function for the integrin alpha 6 beta 4 in the hemidesmosome. *Cell Regul.* *2*, 427–438.
- Kligys, K., Claiborne, J. N., DeBiase, P. J., Hopkinson, S. B., Wu, Y., Mizuno, K., and Jones, J. C. (2007). The Slingshot family of phosphatases mediates Rac1 regulation of cofilin phosphorylation, laminin-332 organization, and motility behavior of keratinocytes. *J. Biol. Chem.* *282*, 32520–32528.
- Langhofer, M., Hopkinson, S. B., and Jones, J. C. (1993). The matrix secreted by 804G cells contains laminin-related components that participate in hemidesmosome assembly in vitro. *J. Cell Sci.* *105*(Pt 3), 753–764.
- Leung, C. L., Liem, R. K., Parry, D. A., and Green, K. J. (2001). The plakin family. *J. Cell Sci.* *114*, 3409–3410.
- Litjens, S. H., de Pereda, J. M., and Sonnenberg, A. (2006). Current insights into the formation and breakdown of hemidesmosomes. *Trends Cell Biol.* *16*, 376–383.
- Margadant, C., Raymond, K., Kreft, M., Sachs, N., Janssen, H., and Sonnenberg, A. (2009). Integrin $\alpha 3 \beta 1$ inhibits directional migration and wound re-epithelialization in the skin. *J. Cell Sci.* *122*, 278–288.
- Mercurio, A. M., Rabinovitz, I., and Shaw, L. M. (2001). The alpha 6 beta 4 integrin and epithelial cell migration. *Curr. Opin. Cell Biol.* *13*, 541–545.
- Nievers, M. G., Schaapveld, R. Q., and Sonnenberg, A. (1999). Biology and function of hemidesmosomes. *Matrix Biol.* *18*, 5–17.
- Nikolopoulos, S. N., Blaikie, P., Yoshioka, T., Guo, W., and Giancotti, F. G. (2004). Integrin beta4 signaling promotes tumor angiogenesis. *Cancer Cell* *6*, 471–483.
- Nikolopoulos, S. N., Blaikie, P., Yoshioka, T., Guo, W., Puri, C., Tacchetti, C., and Giancotti, F. G. (2005). Targeted deletion of the integrin beta4 signaling domain suppresses laminin-5-dependent nuclear entry of mitogen-activated protein kinases and NF-kappaB, causing defects in epidermal growth and migration. *Mol. Cell Biol.* *25*, 6090–6102.
- Osmanagic-Myers, S., Gregor, M., Walko, G., Burgstaller, G., Reipert, S., and Wiche, G. (2006). Plectin-controlled keratin cytoarchitecture affects MAP kinases involved in cellular stress response and migration. *J. Cell Biol.* *174*, 557–568.
- Osmanagic-Myers, S., and Wiche, G. (2004). Plectin-RACK1 (receptor for activated C kinase 1) scaffolding: a novel mechanism to regulate protein kinase C activity. *J. Biol. Chem.* *279*, 18701–18710.
- Palecek, S.P., Schmidt, C.E., Lauffenburger, D.A., and Horwitz, A.F. (1996). Integrin dynamics on the tail region of migrating fibroblasts. *J. Cell Sci.* *109*, 941–952.
- Pulkkinen, L., and Uitto, J. (1999). Mutation analysis and molecular genetics of epidermolysis bullosa. *Matrix Biol.* *18*, 29–42.
- Pullar, C. E., Baier, B. S., Kariya, Y., Russell, A. J., Horst, B. A., Marinkovich, M. P., and Isseroff, R. R. (2006). beta4 integrin and epidermal growth factor coordinately regulate electric field-mediated directional migration via Rac1. *Mol. Biol. Cell* *17*, 4925–4935.
- Rabinovitz, I., and Mercurio, A. M. (1996). The integrin alpha 6 beta 4 and the biology of carcinoma. *Biochem. Cell Biol.* *74*, 811–821.
- Rabinovitz, I., and Mercurio, A. M. (1997). The integrin alpha6beta4 functions in carcinoma cell migration on laminin-1 by mediating the formation and stabilization of actin-containing motility structures. *J. Cell Biol.* *139*, 1873–1884.
- Raymond, K., Kreft, M., Janssen, H., Calafat, J., and Sonnenberg, A. (2005). Keratinocytes display normal proliferation, survival and differentiation in conditional beta4-integrin knockout mice. *J. Cell Sci.* *118*, 1045–1060.
- Reynolds, L. E., et al. (2008). alpha3beta1 integrin-controlled Smad7 regulates reepithelialization during wound healing in mice. *J. Clin. Invest.* *118*, 965–974.
- Riddelle, K. S., Green, K. J., and Jones, J. C. (1991). Formation of hemidesmosomes in vitro by a transformed rat bladder cell line. *J. Cell Biol.* *112*, 159–168.
- Russell, A. J., Fincher, E. F., Millman, L., Smith, R., Vela, V., Waterman, E. A., Dey, C. N., Guide, S., Weaver, V. M., and Marinkovich, M. P. (2003). Alpha 6 beta 4 integrin regulates keratinocyte chemotaxis through differential GTPase activation and antagonism of alpha 3 beta 1 integrin. *J. Cell Sci.* *116*, 3543–3556.
- Santoro, M. M., Gaudino, G., and Marchisio, P. C. (2003). The MSP receptor regulates alpha6beta4 and alpha3beta1 integrins via 14–3-3 proteins in keratinocyte migration. *Dev. Cell* *5*, 257–271.

- Sehgal, B. U., DeBiase, P. J., Matzno, S., Chew, T. L., Claiborne, J. N., Hopkinson, S. B., Russell, A., Marinkovich, M. P., and Jones, J. C. (2006). Integrin beta4 regulates migratory behavior of keratinocytes by determining laminin-332 organization. *J. Biol. Chem.* *281*, 35487–35498.
- Smilenov, L. B., Mikhailov, A., Pelham, R. J., Marcantonio, E. E., and Gundersen, G. G. (1999). Focal adhesion motility revealed in stationary fibroblasts. *Science* *286*, 1172–1174.
- Soosairajah, J., Maiti, S., Wiggan, O., Sarmiere, P., Moussi, N., Sarcevic, B., Sampath, R., Bamburg, J. R., and Bernard, O. (2005). Interplay between components of a novel LIM kinase-slingshot phosphatase complex regulates cofilin. *EMBO J.* *24*, 473–486.
- Tsuruta, D., Gonzales, M., Hopkinson, S. B., Otey, C., Khuon, S., Goldman, R. D., and Jones, J. C. (2002). Microfilament-dependent movement of the beta3 integrin subunit within focal contacts of endothelial cells. *FASEB J.* *16*, 866–868.
- Tsuruta, D., Hopkinson, S. B., and Jones, J. C. (2003). Hemidesmosome protein dynamics in live epithelial cells. *Cell Motil. Cytoskelet.* *54*, 122–134.
- Wiseman, P. W., Brown, C. M., Webb, D. J., Hebert, B., Johnson, N. L., Squier, J. A., Ellisman, M. H., and Horwitz, A. F. (2004). Spatial mapping of integrin interactions and dynamics during cell migration by image correlation microscopy. *J. Cell Sci.* *117*, 5521–5534.
- Zahir, N., Lakins, J. N., Russell, A., Ming, W., Chatterjee, C., Rozenberg, G. I., Marinkovich, M. P., and Weaver, V. M. (2003). Autocrine laminin-5 ligates alpha6beta4 integrin and activates RAC and NFkappaB to mediate anchorage-independent survival of mammary tumors. *J. Cell Biol.* *163*, 1397–1407.